Rotationally Resolved Ground State Vibrational Levels of HC$_2$S Studied by Two-Color Resonant Four-Wave Mixing[†]

Richa Chauhan,[‡] Fabio J. Mazzotti,[‡] Ranjini Raghunandan,[‡] Marek Tulej,[§,‡] Peter P. Radi,[||] and John P. Maier*,[‡]

Department of Chemistry, University of Basel, Klingelbergstrasse 80, CH-4056 Basel, Switzerland, and General Energy Research, Paul Scherrer Institute, CH-5232 Villigen, Switzerland

Received: October 11, 2009; Revised Manuscript Received: November 13, 2009

A high-resolution study of the $\tilde{X}^2\Pi_{3/2}$ ground state rovibronic energy levels of jet-cooled HC$_2$S radical using the double-resonance two-color four-wave mixing technique (TC-RFWM) is reported. The rotational structure of the bands is observed by excitation of selected R-branch lines in the origin band of the $\tilde{A}^2\Pi_{3/2}-\tilde{X}^2\Pi_{3/2}$ electronic system. The second laser frequency is scanned to transfer the population from the rotational level(s) of the upper state to selected vibronic levels of the ground state. Fourteen rotationally resolved vibrational bands have been recorded for energies up to 1800 cm^{-1} above the $v'' = 0$ $\tilde{X}^2\Pi_{3/2}$ electronic ground state. Effective rotational constants and origins are determined for levels that involve fundamental and overtone combinations of the ν_3 (CS stretch), ν_4 (CCH bend), and ν_5 (CCS bend) vibrations. This illustrates the power and advantages of the TC-RFWM approach for the study of the ground state manifold of reactive intermediates produced in low concentrations with high resolution, good signal-to-noise and wide dynamic range.

I. Introduction

The resonant four-wave mixing (RFWM) technique has been recently applied to spectroscopic investigations of charged and neutral species generated in a supersonic discharge.[1–3] The detection limit of $\sim 10^8$ molecules cm^{-3} or lower determined in these studies is comparable to that achieved for laser induced fluorescence (LIF) or cavity ring-down spectroscopy (CRDS) rendering the RFWM technique highly competitive.[1,2,4] Compared to linear methods, the application of RFWM can be advantageous due to complementary capabilities.[2,5] The high signal-to-noise ratio stems from the fully resonant processes involved and from an essentially background-free signal. Furthermore, because the method is based on molecular absorption, it is not dependent on the lifetime of the upper level and is consequently applicable to the detection of predissociative or short-lived excited states.[6–8] The nonlinear character of the coherent method introduces the quadratic scaling of the signal intensity with species number density.[9] This is considered as a limitation of its sensitivity but leads also to a high dynamic range of the RFWM response. RFWM has been exploited in a variety of environments including flames, low-pressure gases and to a lesser extent in supersonic free-jet expansions.[10–12]

The paper presents the spectroscopic study of the ground state energy levels of HC$_2$S radical. It shows that the RFWM can be a superior method for studying the molecular structure in the ground state. From the analysis of the rotationally resolved spectra new structural parameters are determined for a number of vibrational energy levels. The unambiguous spectroscopic assignment can be prepared in a straightforward manner using intermediate level labeling. We show that the approach is applicable to the species present in low concentrations and the

spectra can be measured with a high signal-to-noise ratio due to a fully resonant process. The method is background free in contrast to absorption techniques where a weak signal need to be extracted from a large, fluctuating one. The laser-like signal is detected due to coherent character of the four-wave mixing process and the signal beam can be probed remotely without significant loss, reducing background due to stray light. This approach shows the potential of providing a detailed insight to the spectroscopic pattern in the ground state manifold. An access to high lying energy levels in the ground state can also be useful in studies of the reactive properties of transient species such as unimolecular dissociation.

The investigations discussed here utilize a two-color variant of resonant four-wave mixing (TC-RFWM) resulting in a stimulated emission pumping (SEP) type experiment. Classically, the SEP method is based on optical−optical double-resonance involving two laser beams.[13,14] The first beam (PUMP) transfers population from an initial ground state to a specific level in the electronic excited state while a second beam (DUMP) is used to bring the population back to the ground state manifold. The common SEP detection relies on the competition between spontaneous and stimulated emission by the DUMP laser and results in a small decrease in fluorescence (fluorescence-dip) signal. Only fluorescing molecules can be studied using this technique. In contrast, TC-RFWM does not rely on fluorescing molecules and provides often superior signal-to-noise ratios. The signal is generated by a nonlinear process coupling three input laser beams (2 PUMP and 1 DUMP) that are (i) resonant with two molecular transitions, (ii) share a common (upper) level, and (iii) satisfy the phase matching condition. The double-resonance feature offers a high selectivity for species detection. In addition, intermediate level labeling simplifies complex and congested one-color spectra, allowing precise measurements of line positions and, in most cases, a straightforward assignment of the observed transitions. However, the technique is sensitive to alignment and requires a high quality laser spatial profile as well as good control of beam

intensities to avoid broadening of the molecular transitions due to saturation effects. A variety of theoretical investigations of TC-RFWM can be found in the literature including discussion of the polarization-based schemes and saturation effects.[15–18] The derivation of the signal intensities based on diagrammatic perturbation theory was particularly well tested experimentally.[15,19,39]

The interest in HC$_2$S stems from its importance in interstellar chemistry. A number of sulfur containing carbon chains have been detected by millimeter-wave techniques in star forming regions and in circumstellar envelopes[20] and their importance in understanding physical conditions in these regions was discussed.[21] Although HC$_2$S has not been yet detected in space, it is expected to be an important intermediate for the formation of large sulfur-containing molecules.[22] Two bimolecular reactions are proposed to contribute to the synthesis of HC$_2$S under interstellar conditions: the sulfur cation with acetylene and the carbon dimer with H$_2$S.[22,23]

HC$_2$S has been extensively studied by spectroscopy. Since its first detection via the $\tilde{A}^2\Pi - \tilde{X}^2\Pi$ electronic transition in flash photolysis of thiophene,[24,25] HC$_2$S has attracted considerable attention by experiment and theory. It is an example of a tetraatomic molecule that exhibits a complex coupling of the spin−orbit and Renner−Teller effects. In this context, a number of experimental and theoretical approaches were applied to study the vibrational and rotational structure of this molecule in both the ground and excited state. The ground state structural parameters determined initially from the emission spectra studied in the range 390−450 nm[26] have been improved by millimeter-wave spectroscopy for several vibrational bands including the ν_4 and ν_5 bending modes frequencies.[27,28] The extensive studies by dispersed fluorescence have provided the spin−orbit splitting of 259 cm^{-1} in the ground state and the vibrational energy levels up to 1700 cm^{-1}.[29] The excited state of HC$_2$S was investigated by LIF yielding complex rovibrational structure.[30,31] In parallel, theoretical studies attempted to combine spin−orbit with Renner−Teller interactions to explain the experimental findings.[32,33] Effective Hamiltonian calculations were carried out to shed light on the complex ground state vibrational structure of this radical.[34,35] In model calculations accompanying the LIF studies it has been shown that the large Renner−Teller effect observed in the excited state and the different HCCS and DCCS excited state zero-point spin−orbit splitting can be explained with the assumption of a quasilinear excited state geometry.[31] In spite of considerable advances made in the understanding of the spectral complexity of HC$_2$S, the theoretical approaches developed so far do not offer an unambiguous explanation of all features observed.[33]

In this paper, the structure of the $\tilde{X}^2\Pi_{3/2}$ ground state of the HC$_2$S radical is further characterized by measuring rotationally resolved spectra of vibrational levels by TC-RFWM. Due to the high sensitivity of the method 14 excited vibrational states could be observed in the ground state manifold, 650−1800 cm^{-1} above the v″ = 0 $\tilde{X}^2\Pi_{3/2}$ level. The selectivity of the optical−optical double-resonance method permits an unambiguous assignment based on intermediate level labeling and yields effective rotational constants and band origins.

II. Experimental Setup

The HC$_2$S radical was produced by a slit-jet discharge.[36] The slit length was 30 mm × 1 mm and −1000 V was applied to the electrodes, which were separated by 2 mm. The discharge pulse length was 3−10 μs, resulting in a short but intense pulse of radicals. During the operation of the assembly at 10 Hz, a pressure in the source chamber of approximately 0.05 mbar was

maintained by the vacuum system for a backing pressure of 5−10 bar. The timing between the two lasers, the triggering of the valve and the discharge voltage were controlled by a fast electronic delay generator. These timings are critical for the efficient production of HC$_2$S which was generated by using a C$_2$H$_2$/CS$_2$ (1%/0.5%) mixture in argon as precursor. The optical configuration used has also been described.[3] Two separate Nd:YAG pumped dye lasers were used, one with an intracavity etalon and the other with a double grating. The spectral bandwidth of the two laser sources was around 0.05 cm^{-1}. Frequency calibration was achieved by a wavemeter with an accuracy of 0.002 cm^{-1}. For degenerate four-wave mixing, one of the lasers was split into three components of equal intensities by broadband beam splitters and sent into the vacuum chamber in a BOXCARS configuration.[37] The output energy of the lasers used was attenuated with neutral density filters. In case of TC-RFWM measurements, the third beam was replaced by the output of the second laser (probe or DUMP) and scanned in frequency as the PUMP laser remained at a fixed wavelength. The signal beam, which is coherent and collimated in nature, was separated from the stray radiation by a 6 m detection arm consisting of several irises and spatial filters to obtain nearly background-free spectra. The signal was detected with a photomultiplier. Special masks were used to position the three beam crossing angles (∼1.4°) to satisfy the phase-matching condition $k_1 + k_3 = k_2 + k_4$, where the wave vectors k_1, k_2 (PUMP), and k_3 (probe) generate the signal beam wave vector k_4.[9] The PUMP beams were positioned such that the optically induced fringes were directed along the flow of molecules in the supersonic expansion.[7] The polarizations of the three beams were vertical in the laboratory frame. The signal was digitized by a fast oscilloscope and averaged for 2−3 s for every scan step of the spectrum.

III. Results and Discussion

Initial experiments were performed by applying DFWM spectroscopy on the origin band of the $\tilde{A}^2\Pi_{3/2}-\tilde{X}^2\Pi_{3/2}$ transition of HC$_2$S. The spectrum is reproduced in Figure 1 and shows a well resolved P-branch and a heavily congested R-branch. A least-squares fit to the resolved line positions by means of the PGOPHER program[38] was carried out by constraining the rotational and centrifugal distortion constants
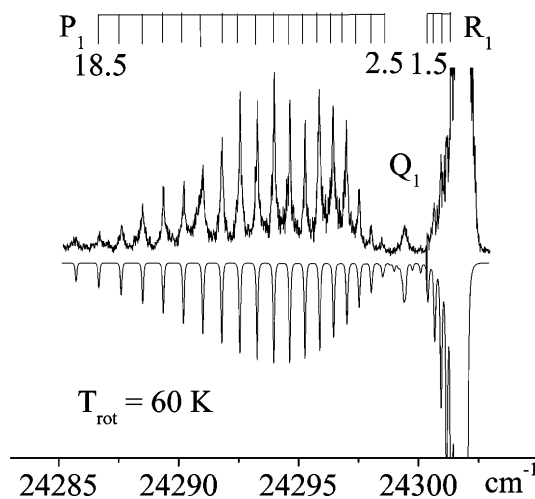

Figure 1. Rotationally resolved DFWM spectrum of the origin band of the HC$_2$S $\tilde{A}^2\Pi_{3/2}-\tilde{X}^2\Pi_{3/2}$ electronic system. The inverted trace is the square of the PGOPHER simulation, assuming a Lorentzian line shape (0.1 cm^{-1} fwhm) and a rotational temperature of 60 K.

Ground State Vibrational Levels of HC$_2$S

J. Phys. Chem. A, Vol. 114, No. 9, 2010 **3331**

of the $\tilde{A}^2\Pi_{3/2}$ state to the values given in ref 26. The spectroscopic constants found in the previous measurement,[21] such as the rotational constant of the lower state, $B_0'' = 0.195\ 693(11)$ cm^{-1} and the origin at $T_{00} = 24\ 299.4430(20)$ cm^{-1} were confirmed. The low J-numbers observed for the jet-cooled radicals prevent an accurate determination of the quartic centrifugal distortion constant, which therefore was fixed at 2.4×10^{-8} cm^{-1}. A simulated DFWM spectrum at a rotational temperature of approximately 60 K is shown inverted in Figure 1. The excellent agreement with the published values validates the procedure for the evaluation of rotational constants and band origins and will be applied in the following for the rotational analysis of higher lying vibrational levels measured by TC-RFWM.

Rotationally resolved double-resonance spectra were obtained by applying the TC-RFWM technique. The pump beams were tuned to known rotational transitions in the 0_0^0 band of the $\tilde{A}^2\Pi_{3/2}-\tilde{X}^2\Pi_{3/2}$ electronic system, exciting well-defined rotational states of the upper level (intermediate level labeling). Subsequently, with the pump laser frequency fixed, the dump (or probe) beam was scanned in the range of selected vibronic bands in the ground state that share a common upper level with the pumped v' = 0 state. Note that the phase matching conditions[9] are met exactly only for one combination of the pump and dump frequencies. Scanning the latter causes a phase mismatch, which reduces the signal intensity. However, in practice, the effect can be neglected and a range of ~900 cm^{-1} is achievable without major realignment.[7] The observed TC-RFWM spectra display excellent signal-to-noise ratios up to ~10^4 for the stronger transitions and allow an accurate determination of line positions. Furthermore, the expected simplification by the double-resonance selection rules reduces ambiguities for the assignment that occur in the one-color spectrum where overlapping transitions are frequently present.

Figure 2 exemplifies the method and the assignment procedure for rotational transitions. The frequency of the pump laser at 24 295.21 cm^{-1} corresponds to the P$_1$(8.5) transition of HC$_2$S in the origin band of the $\tilde{A}^2\Pi_{3/2}-\tilde{X}^2\Pi_{3/2}$ electronic transition. By scanning the probe laser over the same band, we obtain a nearly degenerate two-color four-wave mixing spectrum (upper trace). Alternatively, the probe laser is scanned around 23520 cm^{-1}, addressing the vibrational level of the ground state exhibiting one quantum excitation in ν_3 (lower trace). The resonant lines consist of the P$_1$(8.5), R$_1$(6.5), and R$_1$(8.5) transitions according to the insets in the figure. A minor contribution of a neighboring transition of the pumped P$_1$(8.5) in the origin band is observed in the lower trace. In fact, P$_1$(9.5) is simultaneously excited due to saturation broadening and yields the "satellite" transitions P$_1$(9.5) and R$_1$(7.5) in the 3_1^0 band. TC-RFWM is thus able to characterize the high lying vibrational levels in the $\tilde{X}^2\Pi_{3/2}$ state of the supersonically cooled radical by SEP type approach.

As was demonstrated previously,[3] a convenient way of using TC-RFWM is to tune the pump laser to the band head where numerous rotational levels are excited concomitantly due to overlapping transitions. A scan of the probe laser yields then several resonant transitions to the ground rotational level(s) in a single spectrum. Figure 3 displays an example of TC-RFWM spectra obtained by pumping the band head of the origin transition at 24 301.9 cm^{-1}. For these experiments it is advantageous to remove the intracavity etalon of the laser to broaden the bandwidth to approximately 0.15 cm^{-1} and to excite, therefore, a broad range of P-branch transitions simultaneously
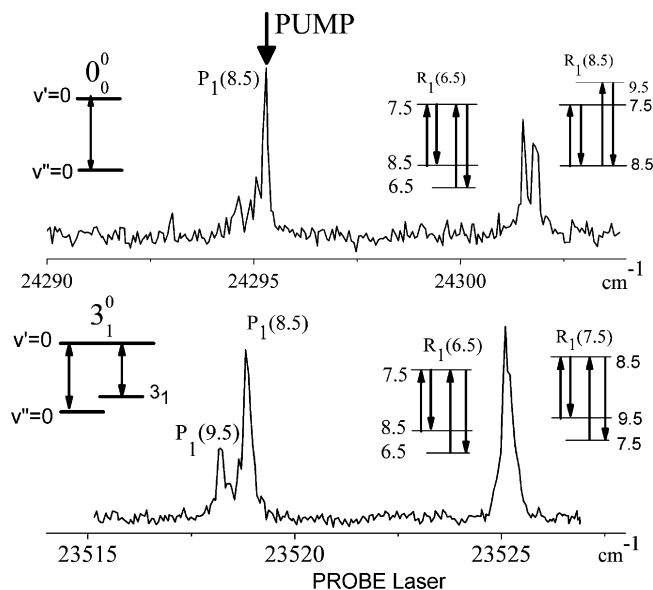

Figure 2. TC-RFWM spectrum. The pump frequency was fixed on the P$_1$(8.5) transition of the origin band of the $\tilde{A}^2\Pi_{3/2}-\tilde{X}^2\Pi_{3/2}$ transition (PUMP). The probe was scanned through the origin (upper trace) and 3_1^0 (lower trace) bands. The nearly degenerate TC-RFWM (upper trace) displays three transitions: the degenerate transition at P$_1$(8.5) and two R$_1$ transitions sharing the upper and lower level (R$_1$(6.5) and R$_1$(8.5), respectively). The SEP spectrum connecting the v' = 0 $\tilde{A}^2\Pi_{3/2}$ state to the 3_1 $\tilde{X}^2\Pi_{3/2}$ level only exhibits two resonant lines that share the common upper level with $J = 7.5$ and v' = 0. The P$_1$(9.5) transition, and R$_1$(7.5) which contributes to the 23535 cm^{-1} peak, are present due to saturation effects (see text).
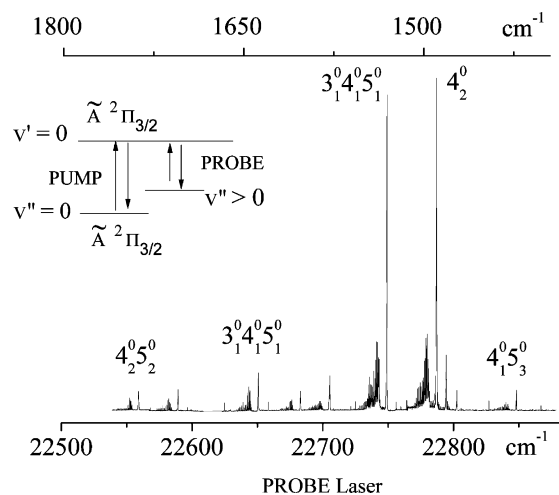

Figure 3. Rotationally resolved stimulated emission spectrum of vibrationally excited ground state levels of the $\tilde{A}^2\Pi_{3/2}-\tilde{X}^2\Pi_{3/2}$ electronic transition of HC$_2$S. The pump laser was set on the band-head of the $\tilde{A}^2\Pi_{3/2}-\tilde{X}^2\Pi_{3/2}$ origin and excites numerous rotational levels simultaneously. The horizontal scale (cm^{-1}) at the top shows the energy above the v'' = 0 $\tilde{X}^2\Pi_{3/2}$. The inset is the scheme of the double resonance approach.

($J = 9.5-21.5$). The subsequent scan of the probe laser in the vicinity of the 5_2^0 band gives rise to a large number of rotationally resolved transitions that are in resonance with the labeled states of the upper level. To avoid power broadening, the measurements have been performed at input intensities below saturation of the molecular transitions. An overview of the TC-RFWM spectrum in the range between 22 500 and 22 900 cm^{-1} is shown in Figure 3.
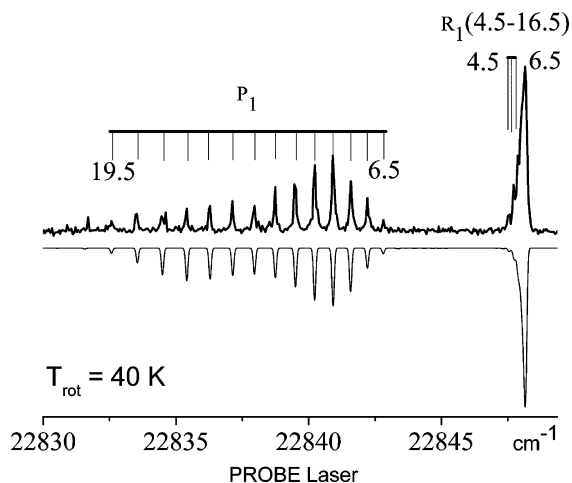
Figure 4. Vibronic structure of the transition detected by TC-RFWM. The pump was set on the bandhead of the origin band in the $\tilde{A}^2\Pi_{3/2}-\tilde{X}^2\Pi_{3/2}$ transition of HC$_2$S. A least-squares fit to the line positions yields the rotational constant and the vibronic origin of the band. A synthetic spectrum with the optimized molecular constants and assuming a Boltzmann distribution for a rotational population at 40 K is shown inverted (see text for details). Intensities are computed by taking into account partial saturation of the transitions.[39]

The $4_1^0 5_3^0$ band around 22 840 cm^{-1} is shown in more detail in Figure 4. The rotationally resolved band structure resembles a $^2\Pi-^2\Pi$ system with a weak Q branch. The assignment of these transitions is straightforward. Intermediate level labeling from the $\tilde{X}^2\Pi_{3/2}$ state by the pump laser yields only transitions to levels in the ground state with the same spin component $\Omega = {}^3/_2$. If ambiguities are encountered for the assignment of specific J-levels, the method described above using a narrow bandwidth laser is applied and yields unambiguous results. The substantial signal-to-noise ratio provides accurate line positions suitable for the determination of effective rotational parameters.

A least-squares fit to the observed frequencies has been carried out using the PGOPHER program[38] and constraining the molecular constants in the $\tilde{A}^2\Pi_{3/2}$ state to the values of ref 26. For each recorded band, two parameters are obtained, B_{eff}'' and the band origin. Around 14 lines were used for the fit of each band. The resulting vibronic origins are determined with a 10% higher precision compared to the previous work by dispersed fluorescence.[29] Furthermore, rotational constants of

the ground state vibrations are determined for 14 vibrational levels of which 12 are reported for the first time. The results are summarized in Table 1. The vibrational assignment and the labeling of the bands (first column) follow the work of ref 29. As can be seen in Table 1, among the five normal modes of the linear molecule, ν_3 (CS stretch), ν_4 (CCH bend), and ν_5 (CCS bend) are obtained from the detected overtones and combination bands. The rotational constants inferred in ref 26 for the two commonly detected ground state vibrational levels (5 and 16) are in agreement with our results to within one standard deviation. However, their tentative assignment of band 16 is in disagreement with the present study. A direct linear trend in the variation of the rotational constant versus the vibrational excitation quantum number is not apparent. The finding is rationalized by considering that Renner−Teller interaction and perturbations may induce a nontrivial potential energy surface along the internal coordinates of the molecule. There are two vibronic bands (4 and 16) for which the rotational constant decrease with respect to the v″ = 0 state (Table 1). The energetically lowest level of them has been assigned as 3_1 and the other as the $3_1 4_1 5_1$ combination.

IV. Conclusion

Double-resonance spectroscopy by TC-RFWM offers a way to access specific vibronic levels of the ground state and to simplify the complex rotational band structure by intermediate level labeling. In the present work, TC-RFWM spectra were recorded and analyzed for the $\tilde{A}^2\Pi_{3/2}-\tilde{X}^2\Pi_{3/2}$ electronic transition of HC$_2$S. These are background-free, show a high dynamic range ($\sim10^4$) and high signal-to-noise ratio for the weakest ro-vibrational bands (~150), enabling their accurate rotational analysis to be made. Rotational constants for selected ground state vibrations with $\tilde{X}^2\Pi_{3/2}$ symmetry were determined by taking advantage of the unambiguous assignment capability of the method. The work reports rotational constants for 14 vibronic bands. With the exception of the constants for the bands 5 and 16 in Table 1, these values are determined for the first time. An uncertainty of 0.005 cm^{-1} improves the values by a factor of 10. The present work combined with the previous results on HC$_2$S should be an incentive for ab initio calculations and a better understanding of the complex and overlapping ground state vibrational structure of this interesting Renner−Teller molecule.

TABLE 1: Spectroscopic Constants Determined for the Vibrationally Excited Levels in the $\tilde{X}^2\Pi_{3/2}$ Ground Electronic State of HC$_2$S[a]

label	T_{0v}	B_{eff}''	B_{eff}'' (ref 26)	residuals ($\times10^{-2}$)	level	$B_{eff}'' - B_0''$ ($\times10^{-3}$)
24	1742.527(13)	0.196140(85)		2.8	$4_2 5_2$	0.45(9)
23	1712.2348(28)	0.197288(22)		0.6	$3_1 4_2$	1.59(2)
20	1650.9168(64)	0.196803(31)		1.6	$3_1 4_1 5_1$	1.11(3)
19	1618.7326(34)	0.196677(16)		0.8	$4_3 5_1$	0.98(2)
18	1596.388(11)	0.195786(53)		2.7	3_2	0.09(5)
16	1552.786(11)	0.195553(52)	0.19558(12)	2.7	$3_1 4_1 5_1$	−0.14(5)
14	1514.7266(77)	0.196683(37)		1.9	4_2	0.99(4)
13	1507.3883(81)	0.196570(55)		1.3	$3_1 5_2$	0.88(6)
12	1499.1669(78)	0.196791(43)		0.9	$4_2 5_2$	1.10(4)
11	1453.5528(37)	0.197119(22)		0.8	$4_1 5_3$	1.43(2)
6	870.334(11)	0.196899(76)		2.5	4_2	1.21(8)
5	822.228(10)	0.195820(45)	0.19595(16)	2.6	$4_1 5_1$	0.13(5)
4	776.4297(66)	0.195537(30)		1.9	3_1	−0.16(3)
2	675.9444(62)	0.19610(40)		1.2	5_2	0.41(4)

[a] The labels and assignments are based on ref 13. All term values and spectroscopic constants are in cm^{-1}. Values in parentheses are one standard deviation.

Ground State Vibrational Levels of HC$_2$S

J. Phys. Chem. A, Vol. 114, No. 9, 2010 **3333**

References and Notes

(1) Raghunandan, R.; Mazzotti, F. J.; Chauhan, R.; Tulej, M.; Maier, J. P. *J. Phys. Chem. A* **2009**, *113*, 13402.

(2) Tulej, M.; Meisinger, M.; Knopp, G.; Walser, A. M.; Gerber, T.; Radi, P. P. *J. Raman Spectrosc.* **2007**, *38*, 1022.

(3) Mazzotti, F. J.; Achkasova, E.; Chauhan, R.; Tulej, M.; Radi, P. P.; Maier, J. P. *Phys. Chem. Chem. Phys.* **2008**, *10*, 36.

(4) Tulej, M.; Meisinger, M.; Knopp, G.; Walser, A. M.; Beaud, P.; Gerber, T.; Radi, P. P. *J. Raman Spectrosc.* **2006**, *37*, 680.

(5) Tulej, M.; Knopp, G.; Beaud, P.; Gerber, T.; Radi, P. P. *J. Raman Spectrosc.* **2005**, *36*, 109.

(6) Tulej, M.; Meisinger, M.; Knopp, G.; Walser, A. M.; Beaud, P.; Gerber, T.; Radi, P. P. *J. Raman Spectrosc.* **2006**, *37*, 376.

(7) Butenhoff, T. J.; Rohlfing, E. A. *J. Chem. Phys.* **1993**, *98*, 5460.

(8) Liu, C.-P.; Reid, S. A.; Lee, Y.-P. *J. Chem. Phys.* **2005**, *122*, 124313.

(9) Vaccaro, P. H. In *Nonlinear Spectroscopy for Molecular Structure Determination*; Hirota, E., Field, R. W., Maier, J. P., Tsuchiya, S., Eds.; Blackwell Scientific: Oxford, U.K., 1998; p 75.

(10) Farrow, R. L.; Rakestraw, D. J. *Science* **1992**, *257*, 1894.

(11) Butenhoff, T. J.; Rohlfing, E. A. *J. Chem. Phys.* **1992**, *97*, 1595.

(12) Radi, P. P.; Tulej, M.; Knopp, G.; Beaud, P.; Gerber, T. *J. Raman Spectrosc.* **2003**, *34*, 1037.

(13) Dai, H.-L., Field, R. W., Eds. *Molecular Dynamics and Spectroscopy by Stimulated Emission Pumping*; World Scientific: Singapore, 1995.

(14) Buntine, M. A.; Chandler, D. W.; Hayden, C. C. *J. Chem. Phys.* **1992**, *97*, 707.

(15) Williams, S.; Tobiason, J. D.; Dunlop, J. R.; Rohlfing, E. A. *J. Chem. Phys.* **1995**, *102*, 8342.

(16) Williams, S.; Rohlfing, E. A.; Rahn, L. A.; Zare, R. N. *J. Chem. Phys.* **1995**, *102*, 8342.

(17) Bracamonte, A. E.; Vaccaro, P. H. *J. Chem. Phys.* **2003**, *119*, 887.

(18) Costen, M. L.; McKendrick, K. G. *J. Chem. Phys.* **2005**, *112*, 164309.

(19) Hung, W.-C.; Huang, M.-L.; Lee, Y.-C.; Lee, Y.-P. *J. Chem. Phys.* **1995**, *103*, 9941.

(20) Gordon, V. P.; McCarthy, M. C.; Apponi, A. J.; Thaddeus, P. *Astrophys. J. Suppl.* **2002**, *138*, 297, and references therein.

(21) Minh, Y. C.; van Dishoeck, E. F. *From Molecular Clouds to Planetary Systems* **2000**, 197.

(22) Yamada, M.; Osamura, Y.; Kaiser, R. I. *Astron. Astrophys.* **2002**, *395*, 1031.

(23) Smith, D.; Adams, N. G.; Giles, K.; Herbst, E. *Astron. Astrophys.* **1988**, *200*, 191.

(24) Krishnamachari, S. L. N. C.; Venkitachalam, T. V. *Chem. Phys. Lett.* **1978**, *55*, 116.

(25) Krishnamachari, S. L. N. G.; Ramsay, D. A. *Faraday Discuss. Chem. Soc.* **1981**, *71*, 205.

(26) Coquart, B. *Can. J. Phys.* **1985**, *63*, 1362.

(27) Tang, J.; Saito, S. *J. Chem. Phys.* **1996**, *105*, 8020.

(28) McCarthy, M. C.; Vrtilek, J. M.; Gottlieb, E. W.; Tao, F.-M.; Gottlieb, C. A.; Thaddeus, P. *Astrophys. J.* **1994**, *431*, L127.

(29) He, S.-G.; Clouthier, D. J. *J. Chem. Phys.* **2005**, *123*, 014317.

(30) Kohguchi, H.; Ohshima, Y.; Endo, Y. *Chem. Phys. Lett.* **1996**, *254*, 397.

(31) He, S.-G.; Clouthier, D. J. *J. Chem. Phys.* **2004**, *120*, 8544.

(32) Perić, M.; Stevanović, L.; Jerosimić, S. *J. Chem. Phys.* **2002**, *117*, 4233.

(33) Perić, M.; Marian, C. M.; Peyerimhoff, S. D. *J. Chem. Phys.* **2001**, *114*, 6086.

(34) He, S.-G.; Clouthier, D. J. *J. Chem. Phys.* **2005**, *123*, 014317.

(35) He, S.-G.; Clouthier, D. J. *J. Chem. Phys.* **2005**, *123*, 014316.

(36) Motylewski, T.; Linnartz, H. *Rev. Sci. Instrum.* **1999**, *70*, 1305.

(37) Prior, Y. *Appl. Opt.* **1980**, *19*, 1741.

(38) PGOPHER, a Program for Simulating Rotational Structure. Western, C.M., University of Bristol http://pgopher,chm.bris.ac.uk.

(39) Bultitude, K.; Bratfalean, R.; Ewart, P. *J. Raman Spectrosc.* **2003**, *34*, 1030.